Republic of Iraq
Ministry of Higher
Education and
Scientific Research
University of Diyala
College of Science
Department of Physics

Synthesis and Characterizations of PPy/ Ag- NiO Nanocomposites and Their Physical Applications

Ph. D. Thesis

Submitted to the Council of College of Science/ University of Diyala in Partial Fulfillment of the Requirement for the Degree of Ph. D. in Physics.

By

Mohammed Ihsan Hasan

B. Sc. 2005

M. Sc. 2011

Supervised By

Prof. Dr.
Nabeel A. Bakr
University of Diyala
2021 A. D

Prof. Dr.
Isam M. Ibrahim
University of Baghdad
1443 A. H.

بِسْمِ ٱللَّهِ ٱلرَّحْمَٰنِ ٱلرَّحِيمِ

﴿ وَتَرَى ٱلْجِبَالَ تَحْسَبُهَا جَامِدَةً وَهِىَ تَمُرُّ مَرَّ ٱلسَّحَابِ ۚ صُنْعَ ٱللَّهِ ٱلَّذِىٓ

أَتْقَنَ كُلَّ شَىْءٍ ۚ إِنَّهُۥ خَبِيرٌۢ بِمَا تَفْعَلُونَ ﴿٨٨﴾ ﴾

النمل الآية (٨٨)

Dedication

This thesis is dedicated to:
To the souls my father and my mother Your love is with me every moment.

My sisters and my brother who motivated me to complete this work.

My wife for helping me throughout this work.
To my lovely three children's

Ihsan, Mesk, and Anas.

Acknowledgments

At first, I thank my God for helping me to finish this work.

I would like to thank the department of Physics in the College of sciences whose giving me the chance to complete this study. Then, I would like to express my appreciation and my deep gratitude to my superadvisors, Prof. Dr. Nabeel Ali Bakr and Prof. Dr. Isam M. Ibrahim who have provided me with confidence and support.

I would like to acknowledge for Professor Sergey Y. Yurish is a president of International Frequency Sensor Association (IFSA) and Sensors Web Portal, Inc. who helped me during my paper submitted steps.

I would also like to extend my special thanks to Eng. Ayed and all my close friends for their help and support.

Mohammed Ihsan

Supervisor Certification

We certify that this thesis entitled **"Synthesis and Characterizations of PPy/ Ag-NiO Nanocomposites and Their Physical Applications"** for the student ***Mohammed Ihsan Hasan*** was prepared under our supervision at the Department of Physics/ College of Science/ University of Diyala as a partial fulfilment of the requirements for Degree of **Doctor of philosophy (Ph.D.) in Physics**.

Signature:
Name: **Professor Dr. Nabeel A. Bakr**.
Title: Professor.
University of Diyala/ College of Science/ Department of Physics.
Date: / / 2021

Signature:
Name: **Professor Dr. Isam M. Ibrahim.**
Title: Professor
University of Baghdad/ College of Science/ Department of Physics.
Date: / / 2021.

In view of the available recommendations. I forwarded this thesis for debate by the Post Graduate Studies Committee.

Head of the department of Physics

Signature:
Name: **Dr. Ammar H. Ayesh.**
University of Diyala/ College of Science/ Department of Physics.
Date: / / 2021.

Linguistic Certification

I certify that the thesis entitled **"Synthesis and Characterizations of PPy/ Ag-NiO Nanocomposites and Their Physical Applications"** prepared by ***Mohammed Ihsan Hasan*** , it has been corrected linguistically. Therefore, it is suitable for debate by examining committee.

Signature:

Name: **Prof Dr. Karim H. Hassan**

Address: **University of Dyiala**

Date: / / 2021

Scientific Amendment

I certify that the thesis entitled **"Synthesis and Characterizations of PPy/ Ag-NiO Nanocomposites and Their Physical Applications"** prepared by ***Mohammed Ihsan Hasan*** , it has been evaluated scientifically. Therefore, it is suitable for debate by examining committee.

Signature:

Name:

Address:

Date: / / 2021

Signature:

Name:

Address:

Date: / / 2021

Examination Committee Certificate

We certify that we have read this thesis entitled **"Synthesis and Characterizations of PPy/ Ag- NiO Nanocomposites and Their Physical Applications"** and, as an examining committee, we examined the student ***"Mohammed Ihsan Hasan***" on its content and in what is related to it, and that in our opinion it meets the standard of a thesis for the Degree of Doctor of Philosophy in Physics.

Signature:
Name: Prof. Dr. Tahseen H. Mubarak
Address: University of Dyiala
Date: / / 2021

Signature:
Name: Prof. Dr. Sabah A. Salman
Address: University of Dyiala
Date: / / 2021

Signature:
Name: Prof. Dr. Ghazi K. Saeed
Address: Wasit University
Date: / / 2021

Signature:
Name:
Ass. Prof. Dr. Ameer F. Abd al Ameer
Address: University of Baghdad
Date: / / 2021

Signature:
Name:
Ass. Prof. Dr. Ulfat A. Mahmood
Address: University of Dyiala
Date: / / 2021

Signature:
Name: Prof. Dr. Nabeel A. Bakr
Address: University of Dyiala
Date: / / 2021

Signature:
Name: Prof. Dr. Isam M. Ibrahim
Address: University of Baghdad
Date: / / 2021

Approved by the council of the college of science.

Signature of the Dean:
Name: Prof. Dr. Tahseen H. Mubarak
Date: / / 2021

Published and Accepted Research Articles

1) Mohammed I. Hasan.; Isam M. Ibrahim. and Nabeel A. Bakr. The Sensitivity of PolyPyrrole NanoTube / (Ag NanoParticle, Ag- NiO nanocomposite) Against H_2S Toxic Gas at Low Temperature. Sensors & Transducers Journal. 2020. 243 (4): 31- 41.
2) Mohammed I. Hasan.; Nabeel A. Bakr. and Isam M. Ibrahim. Morphological, Magnetic, Optical, Surface Potential, and H_2S Gas Sensing Behavior of Polypyrrole Nanofibers. Journal of ELECTRONIC MATERIALS. 2021. (50): 2716- 2724. https://doi.org/10.1007/s11664-021-08790-2.

Abstract

This work focused on the synthesis of three different oxidant- to- monomer (O/M) molar ratios of PPy like a nanofiber structure (PPy NFs), and composite each ratio with (Ag) nanoparticles by the chemical reduction method, it also focused on the preparation of (Ag-NiO) nanocomposite by hydrothermal method, and composite each PPy NFs molar ratio with thus prepared (Ag-NiO) nanocomposite by a volume fraction method. PPy NFs, PPy NFs/ Ag nanoparticles, and PPy NFs/ (Ag-NiO) nanocomposite are investigated by X-ray diffraction, FESEM, and EDS. It was observed that the increases in the $FeCl_3$ oxidant concentration leads to degradation in the Fe^{+3}- MO template structure of PPy NFs.

From the optical properties studies, it was observed that the optical band gap and Photoluminescence behaviour of PPy NFs are changed when increase both of oxidant concentration and (Ag nanoparticles and with Ag- NiO nanocomposite) additions. The thermal stability of PPy NFs increases when the oxidant concentration increases. Surface potential properties of PPy NFs sample shows surface polarization behaviour, and also the oxidant concentration increases may leads to increase in the work function of the PPy NFs. Silver nanoparticles will also seem to enhance the surface potential properties of main surface regions of PPy NFs. M- H curves as results show that the PPy NFs and PPy NFs/ Ag nanoparticles own soft ferromagnetic properties. The response of the H_2S gas of PPy NFs, PPy NFs/Ag nanoparticles and PPy NFs/(Ag-NiO) nanocomposite samples are studied. It was observed that the H_2S gas sensing performance enhanced with the increases in oxidant concentration. H_2S gas response for PPy NFs samples was changed with (Ag) nanoparticles and (Ag/ NiO) nanocomposite addition.

It found also that the largest H_2S gas response is equal to 30.57 % at 25 °C operating temperature with 48.7 and 10.7 seconds response time, recovery time respectively.

The electrical resistance of PPy NFs samples as electrode are changed when the oxidant increases, and by (Ag nanoparticles and Ag- NiO nanocomposite) additions; this leads to change in the electrode conductivity. High CV specific capacitances value is observed in PPy NFs sample, and it is equal to 972.3 F/g.

High CD specific capacitances value was observed in PPy NFs/(Ag-NiO) nanocomposite sample, and it is equal to 512 F/g. Charge- discharge curves of PPy NFs, PPy NFs/ Ag nanoparticles, and PPy NFs/ (Ag-NiO) nanocomposite shows battery and supercapacitor like mechanisms.

List of Contents

Chapter One INTRODUCTION	**Page. No**
1.1 Introduction	1
1.2 Conducting polymers (CPs)	1
1.3 Polypyrrole (PPy)	2
1.3.1 Electrochemical polymerization of PPy	3
1.3.2 Chemical polymerization of PPy	4
1.4 Doping	5
1.5 Template directed growth of conducting polymer nanostructures	6
1.6 Hybrid conducting polymers (HCPs)	7
1.6.1 Synthesis methods of hybrid conducting polymers	8
1.6.1.1 Chemical polymerization of HCPs	8
1.6.1.2 Electrochemical polymerization of HCPs	9
1.6.2 Properties of hybrid conducting polymers (HCPs)	9
1.6.3 Applications of hybrid conducting polymers	10
1.6.3.1 HCPs in sensors	10
1.6.3.2 HCPs as energy storage	11
1.7 Silver NanoParticles	11
1.8 Silver Doped Nickel Oxide Nanocomposite	11
1.9 Thin film preparation	12
1.10 Literature Review	14
1.11 Aim of the work	20
Chapter Two THEORETICAL BACKGROUND	
2.1 Introduction	22
2.2 Crystal Structure of Solids	22
2.3 Polymerization Mechanism of Polypyrrole	22
2.4 Nanofibers Materials	23
2.4.1 Polypyrrole Nanofibers (PPy NFs)	24
2.4.1.1 Mechanism of PPy NFs formation by soft template method	25
2.5 Chemical Reduction Process of PPy	27
2.6 X-ray Diffraction	28
2.6.1 Measurement of X-Ray Diffraction from Thin Film	28
2.6.2 Energy-Dispersive X-Ray Spectroscopy (EDS)	29
2.7 Fourier Transform Infrared Instrument (FTIR)	31
2.8 Filed Emission Scanning Electron Microscopy (FESEM)	33
2.9 Optical Properties	34
2.9.1 Electronic Transition	34
2.9.2 Absorbance	37

2.9.2.1 Optical Band gap	37
2.9.3 Photoluminescence (PL)	38
2.10 Electrical Properties	39
2.10.1 Current-Voltage Characteristics (I-V) Curve	40
2.10.2 Kelvin Probe Force Microscopy (KPFM)	40
2.11 Thermo- Gravimetric Analysis (TGA)	42
2.12 Magnetic Properties	42
2.12.1 Magnetic Hysteresis Loop	43
2.12.2 Polarons - Magnetic Impurity Interaction	45
2.13 Electrochemical Gas Sensor	46
2.14 Energy Storage Device	47
2.15 Electrochemical Properties of Energy Storage Device	49
2.15.1 Electrochemical Impedance Spectroscopy (EIS)	50
2.15.2 Cyclic Voltammetry (CV)	52
2.15.3 Cyclic Charge- Discharge (CCD)	53
Chapter Three EXPERIMENTAL WORK	
3.1 Introduction	55
3.2 Silicon Wafer Substrate Cleaning	56
3.3 Titanium substrate cleaning	57
3.4 The Raw Materials	57
3.5 Chemical Polymerization Method	59
3.5.1 Preparation of polypyrrole nanofibers (PPy NFs) by chemical polymerization method	59
3.6 Additions Methods	60
3.6.1 Preparation PPy NFs/ Ag nanoparticles by the chemical reduction method	60
3.6.2 Preparation Ag-NiO nanocomposite by hydrothermal method	61
3.6.3 preparation PPy NFs/ Ag-NiO nanocomposite by weight percentage method	61
3.7 Material Measurement Techniques and Characterization	62
3.7.1 Structural Measurement Techniques	62
3.7.1.1 X- Ray Diffractometer	62
3.7.1.2 Energy-Dispersive X-Ray Spectroscopy (EDS)	63
3.7.1.3 Fourier Transformation Infra-red (FTIR)	63
3.7.2 Field Emission Scanning Electron Microscopy (FESEM)	63
3.7.3 UV- Visible Spectroscopy	64
3.7.4 Electrical Measurement Techniques	64
3.7.4.1 I- V Characterization	64
3.7.4.2 Kelvin Probe Force Microscopy (KPFM)	65
3.7.5 Thermogravimetric Analysis (TGA)	66
3.7.6 Vibrating Sample Magnetometer (VSM)	66
3.8 Samples Applications	67

3.8.1 Gas Sensing	67
3.8.2 Electrochemical Energy Storage	69
Chapter Four RESULTS AND DISCUSSION	
4.1 Introduction	70
4.2 Structural properties	70
4.2.1 X-Ray Diffraction (XRD) Results	70
4.2.2 Energy Dispersive X-Ray Spectroscopy (EDS)	76
4.2.3 Fourier Transform Infrared (FTIR) Analysis	80
4.2.4 Field Emission Scanning Electron Microscopy (FESEM)	83
4.3 Optical analysis	86
4.3.1 UV- VIS Analysis	86
4.3.2 Photoluminescence (PL)	89
4.4 Thermal gravimetric analysis ((TGA)	92
4.5 Electrical analysis	94
4.5.1 I- V Characteristics	94
4.5.2 Kelvin Probe Force Microscopy (KPFM)	95
4.6 Magnetic Properties	103
4.7 The Gas Sensing Properties	106
4.7.1 Gas Sensor of PPy NFs Mechanism for H_2S gas	107
4.8 The Electrochemical Properties	111
4.8.1 Electrochemical Impedance Spectroscopy (EIS)	111
4.8.2 Cyclic Voltammetry Analysis (CV)	115
4.8.3 Charge- Discharge Curves (CD)	119
Chapter Five CONCLUSIONS and RECOMMENDATIONS	
5.1 Conclusions	123
5.2 Recommendations	124
References	125

List of Figures

CHAPTER ONE	Pages. No
1.1 *Simplified schematic diagram of a conjugated polymer backbone*	2
1.2 *Diaz polymerization mechanism of polypyrrole*	4
1.3 *Chemical polymerization mechanism of polypyrrole*	5
1.4 *Schematic diagram of the microemulsion fabrication of Polypyrrole hollow nanospheres, and their carbon derivative.*	6
1.5 *Schematic diagram of Polypyrrole nanotube fabricated by using reverse microemulsion polymerization*	7
1.6 *Scheme of sol–gel synthesis method*	8
1.7 *Basic mechanisms of emulsion polymerization*	9
1.8 *Classification of thin film deposition methods*	12
1.9 *Schematic diagram of spin-coating method*	13
CHAPTER TWO	
2.1 *Diagram of (a) methyl orange MO molecule, (b) MO–Fe $^{+3}$ fibrillar template Structure*	25
2.2 *MO molecular structure bearing two opposite charges*	25
2.3 *MO–Fe^{+3} template and pyrrole reaction during polymerization routes (I and II)*	27
2.4 *Reportonation of PPy structure during silver ion reduction*	27
2.5 *The Bragg diffraction*	28
2.6 *Principle of Energy-Dispersive X-Ray Spectroscopy (EDS)*	30
2.7 *Component setups of the EDS analysis*	31
2.8 *Working Principle of FTIR spectroscopy*	32
2.9 *Schematic diagram of (FESEM)*	33
2.10 *Electronic energy band gap and chemical structures for PPy (a) undoped, (b) polaron, (c) bipolaron and (d) fully doped states of polypyrrole*	35
2.11 *Diagram of direct, indirect energy band gap*	36
2.12 *Energy- level diagram of a) polaron. b)bipolaron, of PPy*	36
2.13 *Electronic energy levels of the sample and AFM tip for three cases: (a) tip and sample are separated by distance d with no electrical contact, (b) tip and sample are in electrical contact, and (c) external bias (V_{dc}) is applied between tip and sample to nullify the CPD and, therefore, the tip– sample electrical force.* E_v *is the vacuum energy. Level* E_{fs} *and* E_{ft} *are Fermi energy levels of the sample and tip, respectively.*	41
2.14 *Magnetic hysteresis loop of ferromagnetic material*	44
2.15 *Typical magnetic hysteresis loops of soft and hard ferromagnetic materials*	44

2.16 *Two binding magnetic polarons interaction. The polarons are identified by gray circles, small and large arrows show impurity and hole spins, respectively*	45
2.17 *Discharge curves of supercapacitors, capacitors and batteries*	48
2.18 *Schematic representation of the electrochemical double layer*	50
2.19 *Schematic of typical Nyquist plots*	51
2.20 *Cyclic Voltammetry*	52
CHAPTER THREE	
3.1 *Diagram of the preparation method in this work.*	55
3.2 *Diagram of the measurements and applications in this work.*	56
3.3 *Diagram of X-ray diffractometer- 6000 diagram*	62
3.4 *Schematic diagram of FTIR Spectrometer working*	63
3.5 *Schematic diagram of UV–Visible spectroscopy*	64
3.6 *Diagram of I- V circuit*	65
3.7 *Diagram of KPFM circuit*	65
3.8 *Schematic of thermogravimetric analyzer chamber*	66
3.9 *Schematic diagram of vibrating sample magnetometer analyzer system*	67
3.10 *Gas sensor device*	67
3.11 *Gas sensing system*	68
3.12 *Schematic of three- electrode system*	69
CHAPTER FOUR	
4.1 *XRD patterns of M1 and M3 PPy NFs*	71
4.2 *XRD patterns of the M4, M5, and M6 PPy NFs/ Ag nanoparticles*	72
4.3 *XRD patterns of the pure Ag- NiO nanocomposite, M7, M8, and M9 PPy NFs/ Ag- NiO nanocomposite*	73
4.4 *XRD patterns of M10, M11, and M12 PPy NFs/ Ag- NiO nanocomposite*	74
4.5 *EDS analysis of a) M1, b) M2, c) M3, d) M4, e) M5,and f) M6.*	78
4.6 *EDS analysis of a) M7, b) M8, c) M9, d) M10, e) M11, and f) M12*	79
4.7 *FESEM images of a, b) M1, c, d) M2, e, f) M3*	80
4.8 *FESEM images of a, b) M4, c, d) M5, e, f) M6*	81
4.9 *FESEM images of a) M7, b) M8, c) M9, d) M10, f) M11, and e) M12*	82
4.10 *FTIR spectrum of a) M1and b) M2*	83
4.11 *FTIR spectrum of a) M3 and b) M4*	84
4.12 *FTIR spectrum of a) M5, and b) M6*	85
4.13 *FTIR spectrum of pure Ag- NiO nanocomposite*	86
4.14 *a. c) UV- Visible absorbance of M1, M2, M3, M4,M5, and M6. b, d) optical energy gap of M1, M2, M3, M4,M5, and M6.*	87

4.15 *a, c) UV- Visible analysis of M7, M8, M9, M10,M11, and M12. b, d) optical energy gap of M7, M8, M9, M10,M11, and M12.*	88
4.16 *Photoluminescence spectrum of M1, M2, and M3*	89
4.17 *Photoluminescence spectrum of M4, M5, and M6*	90
4.18 *Photoluminescence spectrum of a) M7, M8, and M9, b) M10, M11, and M12*	91
4.19 *Thermal gravimetric analysis of a) M1, b) M2 and c) M3.*	93
4.20 *I-V plot of PPy NFs, PPy NFs/ Ag nanoparticles, PPy NFs/ Ag-NiO nanocomposites samples*	94
4.21 *Surface potential image of the a) M1, b) M2 and c)M3 with (50µm × 50 µm) scanning area and ~ 2 µm tip high at 300K*	96
4.22 *Surface potential image of the M1 at 300K with (17µm × 19 µm) scanning area and ~ 2 µm tip high*	97
4.23 *a) Topological image of M1 at 300K with (1µm × 1 µm) scanning area and ~ (873 nm) tip high. b) surface potential image of M1 at 300K at same conditions*	99
4.24 *a) Topological image of M2 at 300K with (10µm × 10 µm) scanning area and ~ (113 nm) tip high. b) surface potential image of M2 at 300K at same conditions*	100
4.25 *a) Topological image of M3 at 300K with (10µm × 10 µm) scanning area and ~ (211 nm) tip high. b) surface potential image of M3 at 300K at same conditions*	101
4.26 *Work function and electric field of the single PPy NF samples*	102
4.27 *a) Topological image of M4 at 300K with (50µm × 50 µm) scanning area and ~ (2 µm) tip high. b) surface potential image of M6 at 300K with (50µm × 50 µm) scanning area and ~ (2 µm) tip high*	103
4.28 *M- H curves of M1, M2, and M3 at 300K*	105
4.29 *M- H curves of M4, M5, and M6 at 300K*	106
4.30 *Change in the electrical resistance of a) M1, b) M2, c)M3, d) M4, e) M5, f) M6, g) M7, h) M8, and i) M9 with respect to time on the exposure of 30 ppm of H2S gas at 25 ˚C*	108
4.31 *The repeatability curves of M1, M2, M3, M4, M5 and M6 sensor exposed to H_2S at 25 ˚C*	109
4.32 *The repeatability curve of M7, M8, and M9 samples sensor exposed to H_2S at 25 ˚C*	110
4.33 *Nyquist plots of a) M1, b) M2, c) M3, d) M4, e) M5, and f) M6 samples at (0.1 HZ- 1 KHZ) frequency range*	112
4.34 *Nyquist plots of a) M7, b) M8, c) M9, d) M10, e) M11, and f) M12 samples at (0.1 HZ- 1 KHZ) frequency range*	114
4.35 *Cyclic voltammetry of M1, M2, and M3 at 50 mv/s scan rate*	116
4.36 *Cyclic Voltammetry of the M4, M5, and M6 at 50 mv/s scan rate*	117
4.37 *Cyclic Voltammetry of the M7, M8, M9, M10, 11, and M12 at 50 mv/s scan rate*	118

4.38 *Charge- discharge curves of M1, M2, and M3 under (0.01 mA/cm2) applied current density*	120
4.39 *Charge- discharge curve of M4, M5, and M6 under (0.01 mA/cm2) applied current density*	121
4.40 *Charge curve of the M7 samples under (0.01 mA/cm2) applied current density*	121

List of Tables

CHAPTER TWO	**Pages. No**
2.1 *Some of the basic parameters of the battery, classic and electrochemical supercapacitor*	48
CHAPTER THREE	
3.1 *The raw materials of PPy NFs synthesis*	58
3.2 *The raw materials of the nano ddition in this work*	58
3.3 *(MO: Py: $FeCl_3$) molar ratio of PPy NFs samples*	60
3.4 *PPy NFs/ Ag nanoparticles samples*	60
3.5 *PPy NFs/ Ag-NiO nanocomposite sample solutions*	61
CHAPTER FOUR	
4.1 *The diffraction angles, full width half maximum FWHM (Rad) , miller indices hkl, and crystallite size(nm) of the samples*	75
4.2 *EDS analysis of samples*	77
4.3 *Responsivity, response time, and recovery time of samples at room temperature with 30 ppm of H_2S gas concentration*	110
4.4 *The electrode resistance, the electrolyte resistance, the charge transfer resistance, and the electrode conductivity for PPy NFs, PPy NFs/ Ag nanoparticles, and PPy NFs/ Ag- NiO nanocomposite samples with (0.4 cm× 0.4 cm) area of the electrode*	115

List of Abbreviations

symbols	Mean
CPs	*Conducting polymers*
HCPs	*Hybrid Conducting Polymers*
Py	*pyrrole*
PPy	*polypyrrole*
PPy NFs	*Polypyrrole nanofibers*
MO	*methyl orange*
XRD	*x-ray diffraction*
FWHM	*Full width half maximum*
EDS	*Energy-dispersive X-ray spectroscopy*
FTIR	*Fourier Transform Infrared*
FESEM	*Filed Emission Scanning Electron Microscopy*
LOMO	*lower occupied molecular orbitals*
HUMO	*highest unoccupied molecular orbitals*
PL	*Photoluminescence*
KPFM	*Kelvin Probe Force Microscopy*
TGA	*Thermo- Gravimetric Analysis*
HDSC	*High Differential Scanning Calorimetry*
L_e	*electrode thickness*
ppm	*Parts Per Million*
CV	*Cyclic Voltammetry*
CCD	*Cyclic Charge-Discharge*
VSM	*Vibrating Sample Magnetometer*

List of Symbols

Symbols	Mean	Unit
θ	*Diffraction angle*	*Degree*
hkl	*Miller indices*	
D	*Crystallite size*	*nm*
λ	*Wavelength*	*nm*
Wt %	*weight percentage*	
D1	*Thin film thickness*	*μm*
T%	*Transmitence*	
T	*Temperature*	*°C*
α	*Optical absorption coefficient*	
hν	*Energy bandgap*	*eV*
A	*Absorbance*	
I	*Electric current*	*Ampere (A)*
V	*Electric potential*	*Volt (V)*
Φ	*Material work function*	*eV*
$\mathbf{V_{surface}}$	*Surface potential*	*V*
Δψ	*Potential different between tip and sample*	*V*
α	*Positive potential regions*	*V*
β	*High positive potential regions*	*V*
γ	*Negative potential regions*	*V*
δ	*Substrate potential regions*	*V*
E	*Electric field*	$V.\ cm^{-1}$
M	*Magnetization*	$emu.g^{-1}$
H	*Field strength*	*Oe*
R %	*Response of the sensor*	
$\mathbf{R_{air}}$	*Resistances of the sensor in air*	Ω
$\mathbf{R_{gas}}$	*Resistances of the sensor in gas*	Ω
$\mathbf{\sigma_e}$	*Electrode conductivity*	$S.cm^{-1}$
$\mathbf{Z_{real}}$	*Real parts of the complex impedance*	Ω
$\mathbf{Z_{imag}}$	*Imaginary parts of the complex impedance*	Ω
Cs	*Specific capacitances*	$F.g^{-1}$
m	*Active mass of the electrode*	$mg.cm^{2}$
Qs	*Specific discharge capacity*	$mA.\ h.g^{-1}$

Chapter One

INTRODUCTION

1.1 Introduction

Polyacetylene is the first conductive polymer that was discovered by Alan Heeger, Hideki Shirakawa, and Alan MacDiarmid in1977. After this discovery, a variety of conductive polymers were investigated, including polypyrrole (PPy), polythiophene (PT), polyaniline (PANI), poly(3,4-ethylenedioxythiophene) (PEDOT), and poly(p-phenylene vinylene)(PPV) [1]. Conducting polymers show a promising applications in, sensors, battery, supercapacitors, memories, semiconductors, and electromagnetic induction (EMI) shielding [2].

1.2 Conducting Polymers (CPs)

Polymer nanostructures have been synthesized using different techniques, such as soft template methods, hard template methods, and electrospinning technology. Polymers (CPs) such as polypyrrole, polyaniline and polythiophene have a strong electrochemical activity, which makes them valuable for the use of supercapacitors and batteries in the electrode region. The advantages of CPs are low density, corrosion resistance, flexibility, simple morphology control and high conductivity [3- 4]. CPs nanostructures have increased performance in various applications compared to bulk CPs due to their excellent properties such as nanoscale size. CPs are conjugate polymers that have π- bonds on their structure as shown in Figure (1.1), which allows electrons to motivate the whole polymer chain, so that they are CPs can act as semiconductors, magnetic materials and superconductors, and π- electrons delocalization in CPs backbone causes the electrical and optical properties of CPs [5- 7].

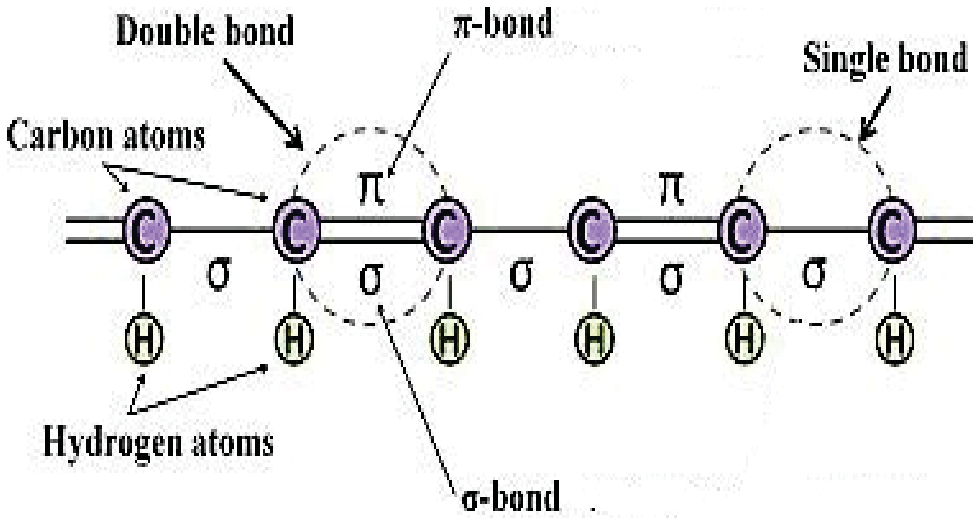

Figure (1.1) Simplified schematic diagram of a conjugated polymer backbone [7].

1.3 PolyPyrrole (PPy)

Pyrrole monomer represent a heterocyclic aromatic organic compound with the formula C_4H_5N, Pyrrole was first discovered by F. F. Runge in 1834.

Polypyrole (PPy) with formula $H(C4H_2NH)nH$ is formed by the polymerization of pyrole monomers, first obtained by Agneli in 1916 from a solution containing pyrole and hydrogen peroxide, first recognized by Mc Nile et al. in 1963, and the first electrochemical preparation of PPy was reported by Dall Olio et al. in 1968, followed by the preparation of a free-standing solution, from this point strong interest in this material led to extensive research into chemical, physical and engineering properties of polypyrrole [8-10]. PPy represents one of the numerous CPs that has been effective in attracting attention due to its specific properties i.e. good environmental and thermal stability, high electrical conductivity and simple synthesis pathway, with many possible applications in the research field of electronic devices such as sensors, batteries, supercapacitors, energy storage and solar cells [11].

Pyrrole polymerization has been suggested to include many reactions including oxidation, deprotonation and crosslinking, for PPy synthesis there are two main processes: electrochemical polymerization and chemical polymerization; pyrrole polymerization occurs in the presence of an oxidant such as $FeCl_3$ or ammonium persulfate; these oxidants are typically used in chemical polymerization [12].

1.3.1 Electrochemical Polymerization of PPy

PPy polymerization method happens rapidly, it is difficult to study this polymerization method step by step; thus, various methods have been suggested to describe the PPy polymerization process [13].

Diaz mechanism is the general method of PPy polymerization, after the pyrrole monomer has been oxidized in figure (1.2a), the cation radical systems in various structures, the electrons where they are not localized only at the nitrogen atoms in the pyrrole ring but also at the carbon atoms as shown in figure (1.2b), the B2 shape reflects the pyrrole cation radicals which are more frequently observed [14].

Two B2 type cation radicals were bonded together as shown in figure (1. 2 c), this is known as α -position coupling, the deprotonation process removes hydrogen atoms then two hydrogen atoms bound at α position with carbon atoms as shown in figure (1. 2 d), and so on in figure (1.2 f) and (1.2 e) [15].

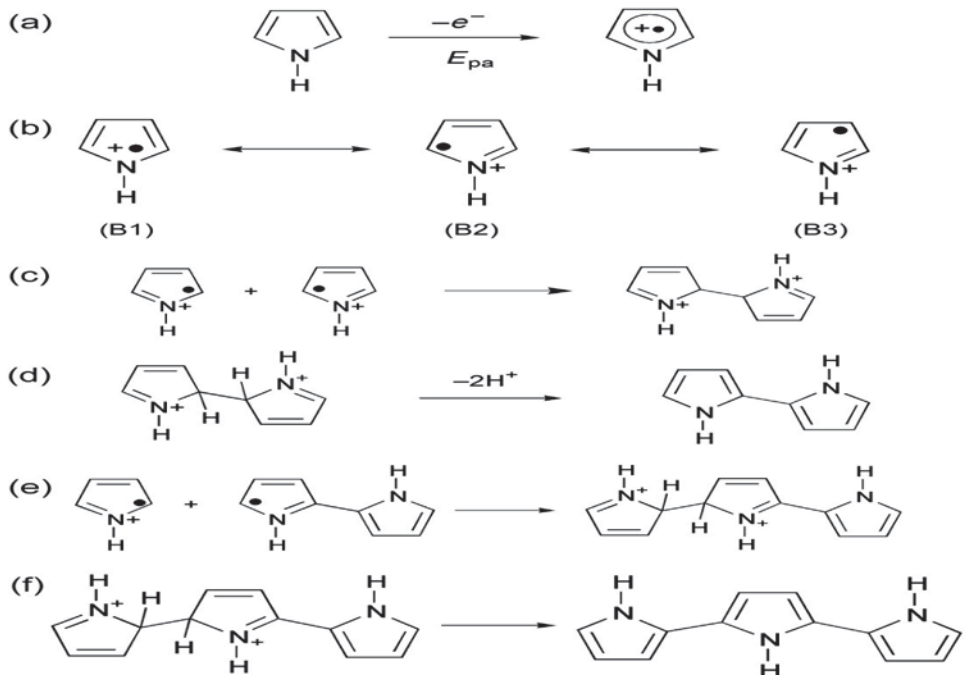

Figure 1.2 Diaz polymerization mechanism of polypyrrole [15].

1.3.2 Chemical Polymerization of PPy

Polypyrrole can be prepared by oxidation of the monomer with chemical oxidants, aqueous $FeCl_3$ is used as chemical oxidants as shown in figure (1. 3) [16].

The conductivity of the PPy depends on a variety of factors, such as: choice of oxidant and solvent, initial monomer-to-oxidant ratio, reaction temperature, etc. which provided the possibility of producing PPy film with high mechanical properties on substrates of any form. Chemical polymerization is a quick and fast process without the need for special equipment and gives a large quantity of powder, so the chemical synthesis seems better for industrial applications [17].

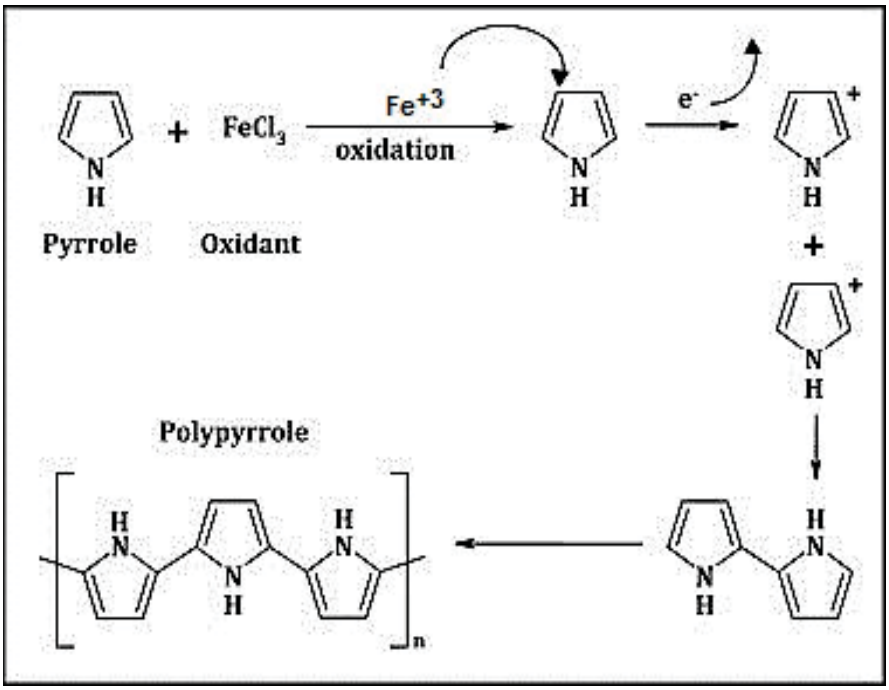

Figure (1. 3) chemical polymerization mechanism of polypyrrole [16].

1.4 Doping

The CPs have been doped using various techniques. Un-doped CPs have been identified as insulators but their electrical conductivity changes from insulating to conductor during the doping process. Doping for CPs is entirely different about what occurs in inorganic materials [18].

The reason for the doping is to remove add electrons to the backbone of the CPs. The oxidation and reduction process produces polarons or bipolars or solitons in the CPs system, which are charge carriers, and the movement of these carriers produces electrical conductivity in the CPs chains. In the p-type doping process, the electron was moved from the highest occupied molecular orbital (HOMO) of the CPs to the doping level, forming a hole in the CPs backbone. But the electrons were transferred from the doping level to the lower unoccupied molecular orbital (LUMO) of the n-type doping CPs, which resulted in an increased electron density [19- 21].

1.5 Template directed growth of conducting polymer nanostructures

Direct growth template producing of CPs includes soft template methods and hard template methods, the first based on the self-assembly of CPs molecules to form various shape nanostructures, while the second methods describe the replicates nanostructure by the chemical interactions [22].

Soft template synthesis, often known as the self-assembly process involves microemulsion polymerization and reverse microemulsion polymerization, microemulsion polymerization generates nanoparticle CPs, these methods can be improved for nanocapsule synthesizing and nanocomposite CPs shape structures. Figure (1. 4) shows fabricated PPy nanospheres by microemulsion polymerization [23, 24].

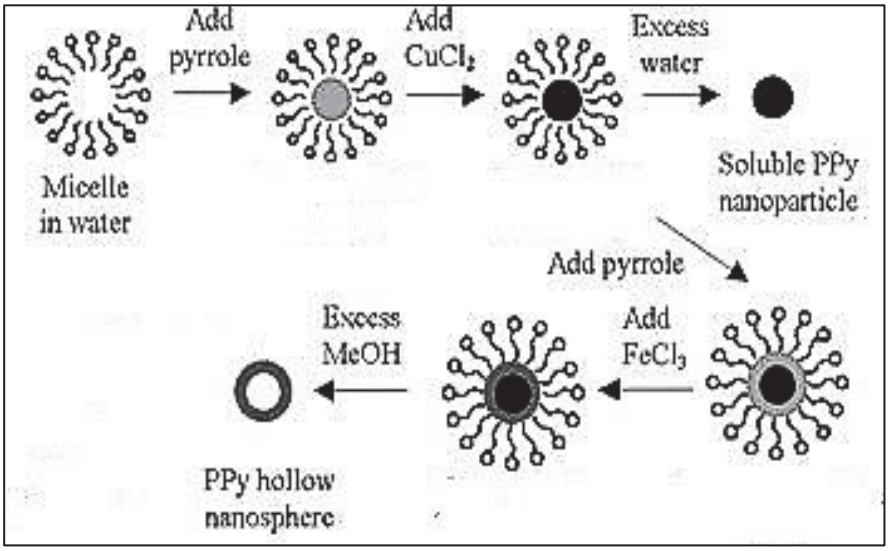

Figure (1. 4) Schematic of the microemulsion fabrication of PPy hollow nanospheres [24].

Reversed-micro emulsion polymerization produces CPs in nanotubes structure by interaction between ions and surfactants, a soft template process having many advantages such as low cost, and useful for the manufacture of large quantities of CPs. Figure (1. 5) show fabricated PPy nanotube by reverse microemulsion polymerization [25, 26].

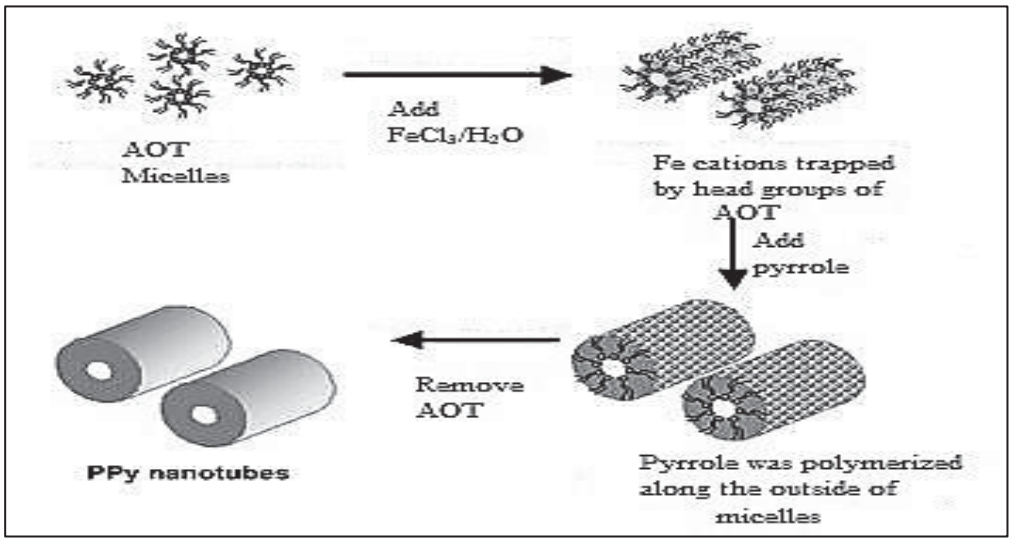

Figure (1.5) Schematic diagram of polypyrrole nanotube fabricated by using reverse microemulsion polymerization [26].

The hard template was used as a scaffold for the growth of CPs. Using nanoparticles as a template, CPs are polymerized on the outer surface of this template, which may result in a core shell structure, and then after removing the template, hollow nanostructures such as nanotubes are obtained. [27]. Soft templates process such as azo-dyes template (representing organic compounds in the functional group R−N=N−R) are introduced to make fibrillar or tubular morphology CPs, which have recently attracted hydrosoluble methyl orange (MO) interest in the preparation of PPy nanofibers or nanotubes [28].

1.6 Hybrid Conducting Polymers (HCPs)

Hybrid CPs are heterogeneous or homogeneous nanocomposite structures, including miscible CPs with organic or inorganic components in which these components are to be measured in nanometers (nm); bonds in HCPs can be divided into two types, weak interactions such as (Van der Waal or hydrogen bonding) and strong interactions such as covalent bonding between the two phases. Successful incorporation of organic or inorganic doping in CP matrices can increase the electron transfer rate [29,30].

The nano hybrid CPs owning excellent physical properties with various application fields such as sensors, battery, and microelectronics [31].

1.6.1 Synthesis methods of hybrid conducting polymers

HCPs can synthesized by the following techniques:

1.6.1.1 Chemical polymerization of HCPs

This technique is used to synthesize HCPs due to fast processing, low cost and various routes. It is divided into two types: polymerization of condensation (polymerization of phase growth) and polymerization of addition (polymerization of chain growth). Sol–gel is a promising technique for the synthesis of HCPs. The formation of HCP occurs through condensation reactions and hydrolysis reactions between CPs and organic or inorganic compounds. The main characteristic for the synthesis of HCPs by the sol-gel method is that CPs and inorganic or organic compounds can be connected together by chemical bonding mechanisms, the diagram of sol–gel method is given in figure (1. 6) [32, 33].

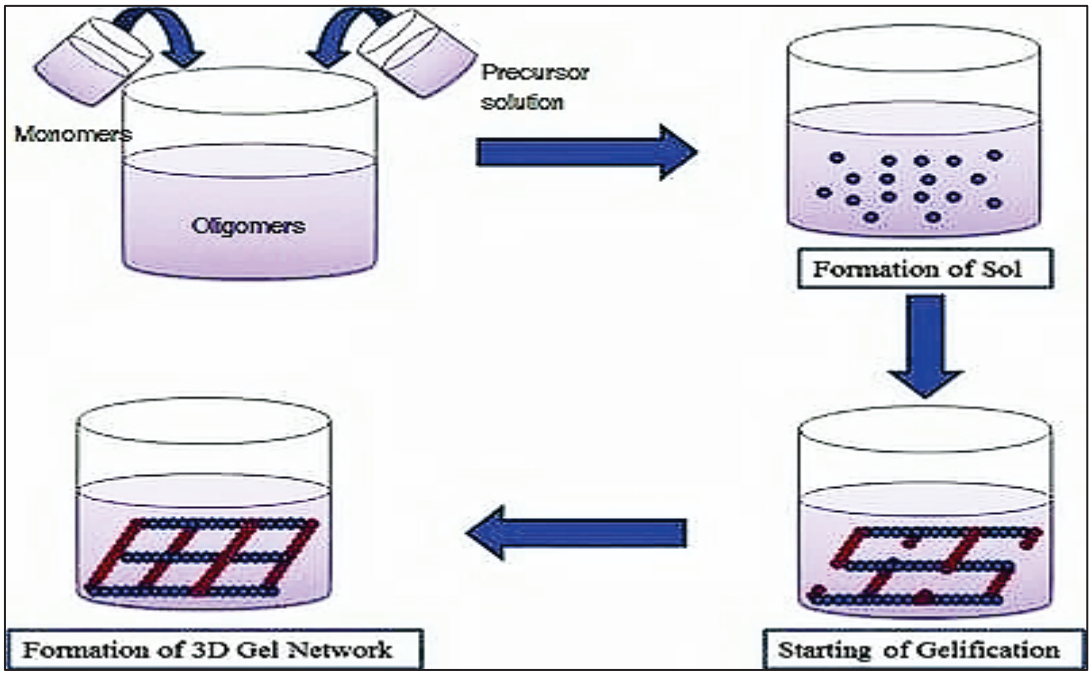

Figure (1. 6) Scheme of sol–gel synthesis method [33].

One of the oxidative methods of polymerization is emulsion polymerization was used for the preparation of HCPs in two types: oil in water and water in oil emulsion. Monomer and surfactant are applied to the solvent when the initiator is added; this causes the formation of micelles and monomer polymerizations associated with these micelles affect the formation in the reaction solution of colloidal dispersions, the emulsion polymerization is shown in figure (1. 7) [34, 35].

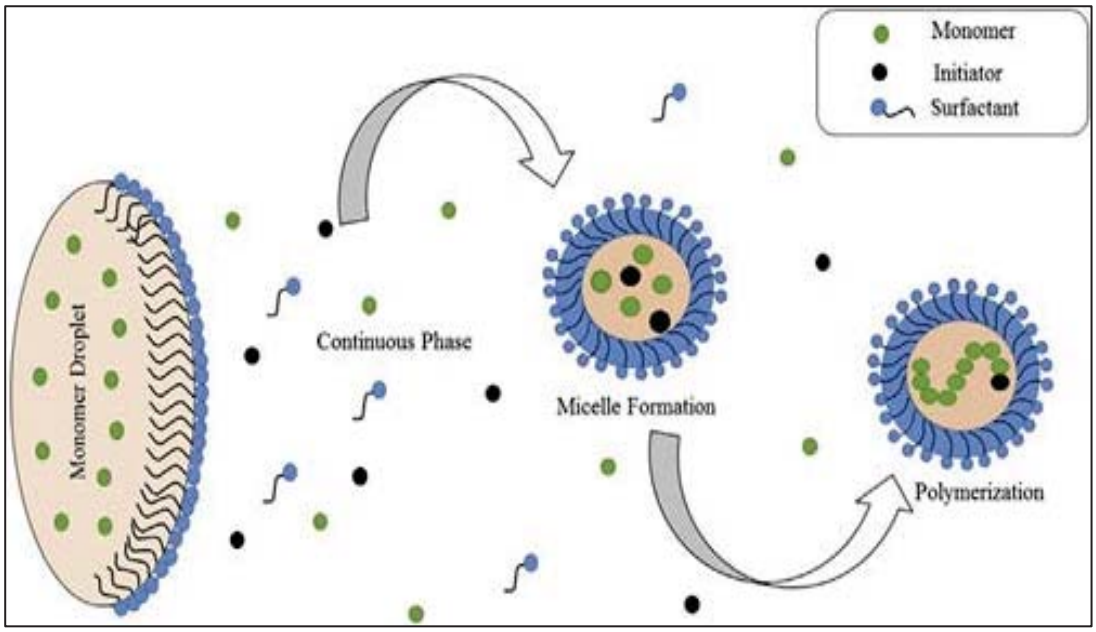

Figure (1. 7) Basic mechanisms of the emulsion polymerization [35].

1.6.1.2 Electrochemical polymerization of HCPs

This technique was used for the preparation of HCPs using three electrodes (reference, working and counter electrodes). Gold, nickel, titanium and platinum are the electrodes used as anodes. Solvents and electrolytes which provide the conductive medium for electrochemical polymerization and dependence on their stability at oxidation potential [36].

1.6.2 Properties of Hybrid Condcting Polymers (HCPs)

The properties of the hybrid conducting polymers depend on the structure, morphological, arrangement of the filler within the CPs matrix and aspect ratio.

The addition of organic or inorganic second filler to the CPs matrix also can increase the physical properties of HCPs. The improvement in conductivity may be due to the uniform dispersion of the filler in the CP matrix. Similarly, the addition of the filler to the HCP matrix increases the thermal properties of the HCPs. Increased mechanical properties of HCPs can be due to additive effects. In addition, the integration of the filler can affect the morphology and structure of the HCPs [37, 38].

1.6.3 Applications of hybrid conducting polymers

In a variety of applications, HCPs can be promising materials including organic electronics, sensors (chemical or biological), energy storage, EMI shielding and biomedicine [39]

1.6.3.1 HCPs in Sensors

HCPs show both the properties of CPs and inorganic materials to be promising material in various applications such as gas and chemical sensors [40]. These properties should be taken into account when choosing gas sensor materials: (1) selectivity, (2) durability, and (3) cyclicability. Selectivity determines whether the sensor is responsible for an analysis group or for a single analysis, stability determines if the sensor can be reproducible over a certain period of time; and the cyclicability determines if the time period of the sensor will operate continuously. The surface area of the HCPs can enhance interactions between the material of the sensor and the analytic, resulting in an increase in analytic sensitivity. The gas sensing properties of HCPs may have been enhanced for the following reasons: (1) the electron mobility of the filler, which helps to increase the charge transport of HCPs and thus enhances the response of the gas sensing system, (2) the large surface area of HCPs helps the adsorption of gas molecules [41, 42].

1.6.3.2 HCPs as energy storage

The electrostatic interaction between the ions in the electrolyte and the charge on the surface of the electrode substrate has been stored in electrochemical capacitors, therefore redox reactions can occur in the electrode material[43].

Recently, a great deal of attention has been dedicated to the use of CPs in electrochemical capacitor applications and stored electrochemical batteries[44]. CPs such as PPy have been usually used as active electrode material in energy storage applications, but have poor stability; therefore this problem can be overcome by manufacturing HCPs. [44, 45].

1.7 Silver NanoParticles

Silver may be engineered into nanoparticles form, the silver nanoparticle was ranged from 1 to 100 nm in size. Owing maximum surface area; this leading to the highest values of the weight ratio. Silver nanoparticles were obtained by various synthesis such as electron irradiation, photochemical methods, laser ablation , and chemical methods including chemical reduction method for CPs reducing agents and electrochemical techniques [46].

Several reducing agents play a role in the formation of metal salts into metal nanoparticles. Most of these reducing agents need temperature during chemical reduction but some reducing agents will reduce to nanoparticles at room temperature [47].

1.8 Silver doped Nickel Oxide Nanocomposite

Nickel oxide (NiO) is an important semiconductive metal oxide used as electrodes, sensors and electronic devices. Nickel oxide is used as a reinforcement material during the preparation of CPs due to their unique properties, often the discovery of Ni^{+} and Ni^{++} ions in nickel oxide can enhance the motivation of the charge carrier through the CPs. [48].

Noble metals represent a great deal for improves properties of NiO. Silver is one of the noble metals with the lowest price and good properties has been used usually in NiO doping, silver- nickel oxide nanoconposite materials have shown excellent electrical conductivity performances for sensor and other devices, so that the incorporation of Silver- Nickel Oxide nanoconposite in polypyrrole matrix was enhanced the doping process; this leads to the best physical properties [49].

1.9 Thin film Preparation

Thin film technology plays an important role in the industry, and is generally used for the preparation of integrated circuits. However in the industry request to the production of smaller integrated circuits with advanced materials at higher speeds, while new processing techniques have emerged [50]. Thin film techniques during the 20th century have required for a wide range of technological advances in many fields such as: magnetic recording, semiconductor devices, LEDs, cutting equipment, and (solar cells) storage (fine-film batteries or supercapacitors).Figure (1. 8) represents the generally thin film deposition methods techniques [51].

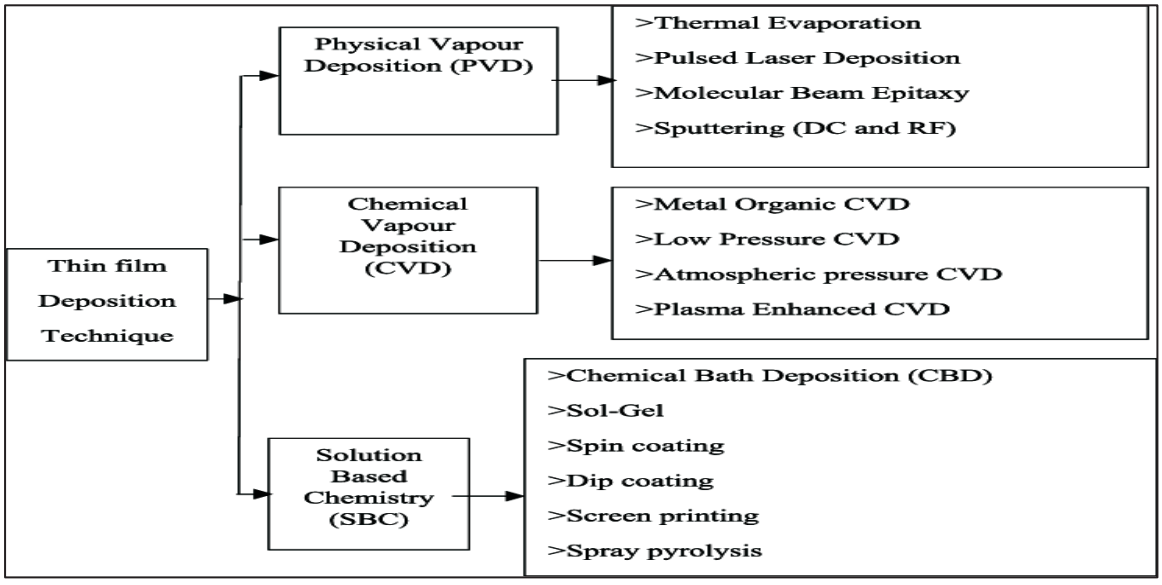

Figure (1. 8) classification of thin film deposition methods [51].

For deposit uniform thin film onto sample substrate, amount of coat material was added to non-spinning substrate, after that the substrate rotated up to 1000 rpm to distribute the material by centrifugal force [52]. The thickness of the film depends on various factors such as concentration of the solvent and its viscosity [53]. The surface tension and the viscous force represents the key causes of the deposition material on the substrate, the spin coating technique involves several steps such as spin on , fluid distribute, evaporation, spin off, respectively as shown in figure (1. 9) [54].

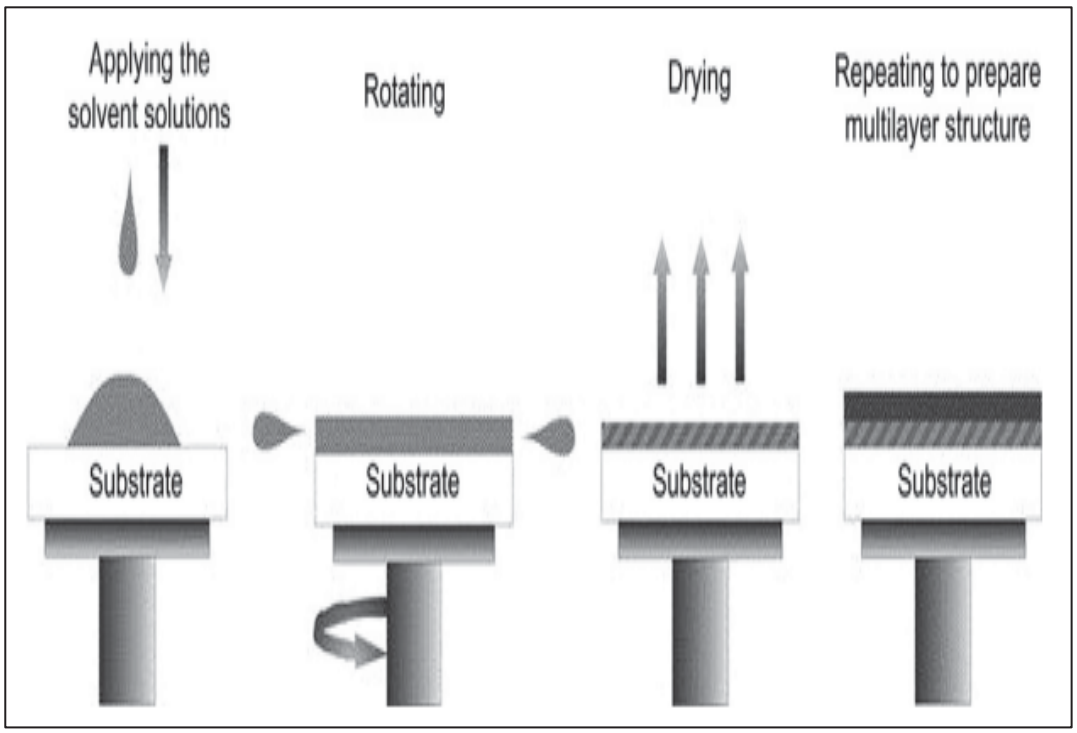

Figure (1.9) schematic diagram of spin-coating method.

Spin coating method has several advantages: it is a simple technique that can be prepared at room temperature, and low cost to manufacturing thin films, spin coating method is the best technique to produce thin films with uniform thickness ranging from 0.4 to 5.0 μm on the small substrate surface [55].

1.10 Literature review

Yang et al. in 2005 offer a process that is estimated the pyrrole (Py) polymerization on the surface of methyl orange- iron(III) chloride (MO–$FeCl_3$) complex template. (1.5 mM) of $FeCl_3$ and (0.15 mM) of MO were dissolved in 30 ml of deionized water solution. Then (1.5 mM) of Py was added to the above ($FeCl_3$- MO) solution and stirred at room temperature for 24 hours. PPy precipitate washed several times with deionized water and ethanol and finally dried under a vacuum at 60 °C for 24 hours.The PPy tubular structure was confirmed by the TEM micrograph, where the hollow nanotube diameters are approximately 50 and 70 nm, respectively. Complexation between organic compounds such as dye and Fe^{+3} is found to be very effective. $FeCl_3$ act as a flocculant, in chemistry. MO in water-soluble has anionic properties in an aqueous solution, and having a planar hydrophobic part and hydrophilic edge ($-SO^{-3}$). $FeCl_3$ can remove electrostatic repulsions between MO aggregations that react in solutions with negatively charged of MO aggregates, and form an amorphous complex [56].

Gonçalves et al. in 2006 reported the relationship between $FeCl_3$ oxidant - to-pyrrole monomer molar ratio and study the electrical conductivity of polypyrrole according to these different oxidant concentration (increasing oxidant- to-monomer molar ratio from 1.4:1 to 2.8:1). PPy formed by chemical polymerization of Py by using $FeCl_3$ as an oxidant. Py kept at 6 ºC before use, the reaction solution was stirred for 2 hours, then filtered, washed and dried at 50 ˚C for 12 hours. PPy used as a cathode layer and the electrical conductivity for a molar ratio of 2:1 equal 7.5 S/cm due to the limited amount of oxidant used which could not oxidize all the existing monomers [57].

Johnston et al. in 2006 show that PPy coated fibers can be obtained by method of Py dispersion polymerization (cellulose fibers, monomers, and additives are dispersed into water) then $FeCl_3$ is added to the oxidizing solution. A fully distributed suspension of individual cellulose fibers is available in dry pulp in 500 mL of water. It was filtered and the fibers were re-distributed by stirring (0.5 M) pyrrole and (0.05 M) of sodium benzene-sulphonate dodecyl in 500 mL water solution for 1 h to allow pyrrole to penetrates the surface cellulose fibers. After that the fibers were filtered and washed with a pyrrol solution, (0.5 M) of $FeCl_3$ which was added as a polymerization oxidant. The suspension was then left for 3 hours to make sure it was polymerized. The resulting PPy- coated cellulose fiber was filtered and washed thorough the sieve with distilled water to remove any free PPy. The coated fibers were then re-dispersed in ethanol and washed with water. The electrical conductivity of these composites was greatly enhanced over those of the precursor fibres [58].

De Melo et al. in 2007 were showed that polypyrrole (PPy) can be used as a sensor for certain components in gas, such as inorganic (NH_3) and organic molecules (acetone, methanol, and ethanol). Primarily, 4% of the solution of PMMA+, PTSA, PCP, PEO, and PVAC was dissolved in a (0.05M) solution of ferric chloride into an exact solvent such as tetrahydrofuran (THF), chloroform, water, and methanol, respectively. Subsequently, a limit quantity of these polymer solutions with ferric chloride was deposited on ITO substrate. These polymeric film was exposed to a vapor Py for (30 min) resulting in the polymerization of the Py monomer occurs, and PPy structure has been blended with the above conventional polymer chains, the polymerization of the PPy chains occurs not only on the outer surface of the film, but also around all $FeCl_3$ grains distributed in the above conventional polymer matrix [59].

Yun et al. in 2007 synthesis of polypyrrole nanotubes (PPy NTs) using the ($FeCl_3$- MO) fibrillary complex as a template. The complex template could begin pyrrole monomer polymerization and PPy growth as nanotubes, and the ($FeCl_3$-MO) template was self-degraded after (Py- MO- $FeCl_3$) reaction, leaving PPy NTs at high yield [60].

Hernandez et al. in 2007 used PPy a single nanowire coated on gold electrodes and deposited on a microfabricated SiO_2/Si substrate to use this method for the detection of NH_3 gas. It was also used for the gas response to NO_2, but did not demonstrate any gas sensitivity to this analyte [61].

Shubhra et al. in 2009 used PPy Nanofibers with (HCl, p-TSA, $FeCl_3$, CSA, and PSSA) dopants to synthesize PPy nanofibers, this oxidative polymerization method is used to produce PPy nanofibers. For the purpose of the doping process, 2M are dissolved in 20 ml of water each dopants. 3.2 mM APS was used as an oxidizer to the solution of each compound. (12.8mM, 0.87ml) pyrrole monomer dissolved in 40 ml of chloroform. The pyrrole solution then added drop-wise. At room temperature, the reaction mixture remained unchanged. The polymerization reaction was stirred for 15 minutes for each set. Then, the precipitate was filtered and washed with acetone and distilled water to extract impurities. At room temperature the black powder was finally vacuously dried for 24 hours. As result the electrical conductivity polypyrrole nanofiber depends on the doping (p-TSA > CSA > HCl > $FeCl_3$ > PSSA) [62].

Marchesi et al. in 2010 investigated small contents of iron in PPy matrix, the iron was incorporated in PPy matrix which origin from adding of $FeCl_3$ to the reaction solution during the chemical pyrrole monomers polymerization. Relationship between PPy pellets with the addition of $FeCl_3$ lead to increase the saturation magnetization (M_s) of PPy and the ferromagnetic state of PPy was observed when iron element is present in this material.

This increase in the magnetic saturation due to the presence of iron species in PPy matrix can be related to locally polarized polarons generating an increase in the effective saturation magnetization as suggested by das sarma for magnetic semiconductor theory explained [63].

Xiaoming et al. in 2010 synthesized PPyNFs with a simple process of reactive template. The reactive $FeCl_3$ template with MO provided stable PPy NFs. The ammonia gas sensor was based on polypyrrole shows a higher sensing performance than the ammonia gas sensor was based on polypyrrole nanofiber [64].

Kwon et al. in 2010 synthesized PPy nanoparticles with nanodiameter sizes (20 and 60 nm) by pyrrole chemical oxidation polymerization. Polyvinyl alcohol (PVA) was dissolved in water and reacted with metal cations of $FeCl_3$ in water and formed complex compounds. PPy nanoparticles (PPy NPs) of different diameters could be acquired under the following experimental conditions, PVA aqueous solutions have been added to $FeCl_3$ and $FeCl_3$ has a molar ratio of 2.3 to pyrrole. When monomer is already in contact to the oxidizing agent immediately polymerizing continues. Within few minutes the solution was black and mixed for a minimum of 2 hours. PPy NPs were later washed with distilled water several times to remove impurities and dried under vacuum for 24 hours at room temperature. The smallest (20 nm) PPyNPs was used as sensor to provide the full sensitivity of NH_3 [65].

Nurul et al. in 2011 prepared (NiO–PPy) composite electrodes for Li-ion batteries by the chemical polymerization of pyrrole with sodium p-toluenesulfonate and Triton-X as doping and surfactant, respectively. Cauliflower-like PPy particles formed with a uniform NiO coating. The electrochemical results for the NiO–PPy composite have been improved

compared to the pure NiO. After 30 cycles, the capacities for pure NiO is about 119 mA.h/g and for NiO–PPy composite about 436 mA.h/g [66].

Yuan et al. in 2011 studied The relationship between the oxidant-to-monomer molar ratio of $FeCl_3$ and the electrical conductivity of PPy by increasing the oxidant-to-monomer molar ratio from 0.25:1 to 2.5:1. The reaction solution was stirred for 1 hour, then filtered, washed and dried at 75 C. The results showed that the conductivity of PPy was dependent on the oxidant-to-monomer molar ratio and that the maximum value for electrical conductivity of PPy was equal to 15 S/cm at 0.75:1 mole ratio [67].

Ramesan et al. in 2012 synthesized PPy composite by chemical oxidative polymers with CuS NPs of the copper sulfides. A thioacetamide- CTAB solution was added with a continuous stirring to the copper acetate solution for 20 minutes at 30˚C. After 12 hours, the brown solution became green (50 to 300 nm) of the copper sulfide nanoparticular has been obtain. (0.03M) pyrrole in 50 ml of distilled water with copper sulfide nanoparticular solutions have been ultrasonicated for over 35 min. (0.06M) APS added to sulphide particle dispersion in solution and stirred at 10°C, when changing to a black color, this indicating to reaction had polymerization immediately. The polymerization was carried out with continuous mechanical stirring for 9 hours at room temperature PPy/CuS nanocomposite precipitate was filtered and washed with methanol and distilled water on various times. At 60 ˚ C for 24 hours, the processed powder was dried. PPy has improved its electrical conductivity by increasing the number of CuS NPs in the PPy matrix and this may be due to the interactions between CuS and the polymer component [68].

Jitka et al. in 2013 prepared PPy NTs by polymerization of Py with $FeCl_3$ (1:1) molar ratio in the presence of MO molecules. Then PPy NTs is used to reduce Ag NPs from the $AgNO_3$ aqueous solution. The results indicated to nanotube

shape of PPy. The presence of silver nanoparticles has had an effect on electrical conductivity [69].

Joulazadeh et al. in 2015 prepared PPy NTs using a complex methyl orange (MO) and iron (III) chloride ($FeCl_3$) template. The effect on the final PPy NTs morphology of molar reactants ratios (Py:MO:$FeCl_3$). The results showed that the high pyrrole monomer amounts could degrade the template and form a hollow tubular shape, while the presence of a low pyrrole amount could lead to non-hollow fibrillar morphology. It is expected that the relative molar relation of MO: $FeCl_3$ will be relevant for formulating nanostructures based on templates [70].

Xiang et al. in 2015 used PPy– nanocomposite graphene decorated as sensitive surface for NH_3 by TiO_2 NPs added. Pyrrole, CTAB and citric acid (0.1 M) were dissolved in deionized water and then stirred for 3 hours. (0.5 M) APS dissolved in 20 ml of deionized water, then added for 0.5 h into the prepared solution and stirred for 4 hours, then the solution was filtered and washed with methanol and deionized water and dried at 60 °C, this lead to obtaining PPy-graphene nanocomposite. TiO_2 nanoparticles were decorated using the Sol–gel method with PPy–graphene nanocomposite. The solution was dried for 10 hours at 70°C. 0.1 g of PPy- graphene nanocomposite/ TiO_2 powder dissolved in 5 ml of (DMF) solution with ultrasonicated for 0.5 h, the solution syringed on the space between the two copper foils strip and dried. The response of PPy-graphene nanocomposite/ TiO_2 NPs for 50 ppm ammonia was 102.2 per cent at room temperature [71].

Joulazadeh et al. in 2015 used PPy NFs for the detection of propanol, methanol, butanol, and ethanol. PPy NFs sensor showed higher response to propanol and butanol this is may be due to the longer alkyl chain compared with ethanol and methanol [72].

Jamalabadi et al. in 2018 successfully prepared and deposited PPy- (NiO, SnO_2-NiO, ZnO-NiO, and WO_3,) hybrid nanocomposite thin films by electrospinning technique. The sensing performance have been studied when these thin films were exposed to methyl-, ethyl-, dimethyl-,and propylamine, acetone, ethanol, and water vapors. The results showed the ability for quantification of different amine vapors at low temperature in humid atmosphere [73].

Ramesan et al. in 2018 prepared PPy/ (Ag-NiO) nanocomposites by polymerization of Py with different contents of Ag/ NiO nanocomposites. PPy/ Ag-NiO nanocomposites showed an improvement for high sensitivity detection towards ammonia gas than pure PPy [49].

Mahdi et al. in 2018 presented the composite thin films of polypyrrole (PPy) with functionalized single wall carbon nanotube (fSWCNT) for hydrogen sulfide (H_2S) gas sensing application. The response of these composite films for H_2S gas was evaluated by monitoring the change in electrical resistance at (20, 50, 100, 150 and 200) $^{\circ}$C. It was observed that the PPy/ fSWCNT nanocomposite films show a higher sensitivity as compared to pure PPy [74].

1.11 Aim of the work

- Syntheses of polypyrrole nanofibers with different oxidant/ monomer ratio by using soft template method and using PPy NFs to reduction of Ag nanoparticles from silver nitrate aqueous solution.
- Syntheses of (Ag- NiO) nanocomposites by using hydrothermal method and preparation of PPy NFs with (Ag- NiO nanocomposites) by using volume fraction method.
- Study the effect of oxidant and additions on the structural, optical, electrical, magnetic and electrochemical behaviour of PPy NFs. And using PPy NFs with addition in some application such as gas sensing and like energy storage device.